Architecture Considerations for 60 GHz Wireless Networks

Candy Yiu
Department of Computer Science
Portland State University
Portland, OR 97207
Email:candy@cecs.pdx.edu

Suresh Singh
Department of Computer Science
Portland State University
Portland, OR 97207
Email:singh@cecs.pdx.edu

***Abstract*—Providing high data rates to wireless users has long been a goal that has driven the development of new technologies and standards in the past decade. Now, with the opening up of the spectrum at 60GHz, it has become possible to design WLANs that can meet the goal of Gbps/user connectivity. This paper examines several unique design challenges brought about because of the physical characteristics of this frequency band. We show that antenna geometry has a significant impact on throughput. This result is obtained when we utilize realistic 3D beam patterns, rather than the common 2D approximation. Indeed, the maximum average throughput for a linear antenna array of 8Gbps (using only 640MHz of spectrum) is more than double that obtained with a circular array consisting of the same number of antenna elements. We explore the challenge of providing coverage in dead spots using the novel idea of passive reflectors.**

I. Introduction

The opening of the 60GHz ISM (Industrial Scientific Medical) band has triggered intense interest in industry as well as academia on how best to exploit the available 5-7GHz bandwidth. From a network design point of view, this frequency band offers a specific challenge not seen at lower ends of the spectrum (for instance the bands we are more familiar with, between 2-5GHz). At 60GHz, the signal attenuation is high because of oxygen absorption and absorption by many materials commonly used in construction. Therefore, reflected components of a signal tend to be significantly attenuated as compared to a direct path. Furthermore, given the high frequency, there is also significant attenuation with distance (88 dB/10m as compared with 60 dB/10m for 2.5 GHz). Therefore, as [5] points out, technologies such as MIMO (Multiple Input Multiple Output) that rely on a rich multipath environment are not useful at this frequency. Indeed, typical WLAN architectures used at lower frequencies (which exploit multipath) are not suitable for 60GHz networks. This leads to the design challenge of how best to architect WLANs at this frequency so as to provide high data rate coverage indoors.

The approach proposed by various authors is to build a WLAN around the idea of highly directional smart antennas at the access points (AP) and users. The benefit of these antennas is the high gain and adaptive beamforming. But the drawbacks are many. For instance, links can be easily broken by obstacles as the user moves behind an obstruction or if another person comes in the Line of Sight (LoS) path between the user and AP (the high water content of the body is a very good absorber of this frequency).

In this paper we examine various design tradeoffs in designing a 60 GHz WLAN. A key aspect of such a WLAN is the choice of antenna configurations at the AP and users. We analyze the obtainable network throughput when using two different antenna array geometries (linear and circular). The choice of antennas affects the allocation of spatial channels which in turn impacts the network throughput as described in section III. The results presented are based on detailed Matlab simulation of the propagation environment and antenna models. The throughput analysis is then extended to the problem of maintaining link reliability in the face of user mobility and dead spots caused by obstructions in section IV. Related work is presented in the next section.

II. Related Work

60GHz is well-absorbed by oxygen in the atmosphere and by several materials [8], [4], [5], [3], [7] leading to the absence of a rich multipath environment. Thus, LoS paths are the predominant signal path and due to the severe attenuation of reflected signals, this part of the spectrum is well-suited to highly efficient spatial frequency reuse. [2] reports on propagation measurements at 60GHz and 2.5GHz. They note that large-scale propagation for 60GHz can be modeled as free space (a measured path loss exponent of 2.1 in buildings) as was also noted by [1]. Other results of these and other measurement studies [11] note the small RMS delay spread for 60GHz indicating little multipath. [12] presents a detailed measurement study of 60GHz propagation in indoor environments with particular attention to multipath. One interesting result is that the strongest reflected components (polished surfaces) are at least 10dB below the LoS component. Second-order and higher-order reflections are highly attenuated and negligible. Penetration loss through walls in the building are very high with many examples of over 35dB.

[9] presents a MAC design for a *multihop* 60GHz WPAN. Every node uses highly directional antennas and high transmit power to maintain a network-wide rate of 2Gbps. However, the paper assumes diffraction at this frequency band (not supported by measurements) and does not consider the attenuation

due to different materials that may obstruct the signal path (including the human body).

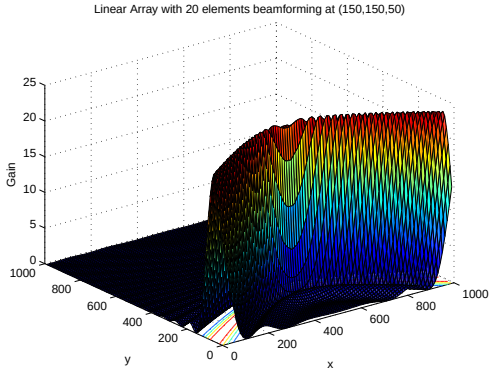

Fig. 1. Gain with 20-element linear array pointing to (1.5m,1.5m,0.5m) and the axis of the antenna aligned along the y-axis.

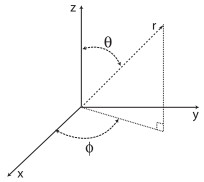

Fig. 2. 3D angle convention used.

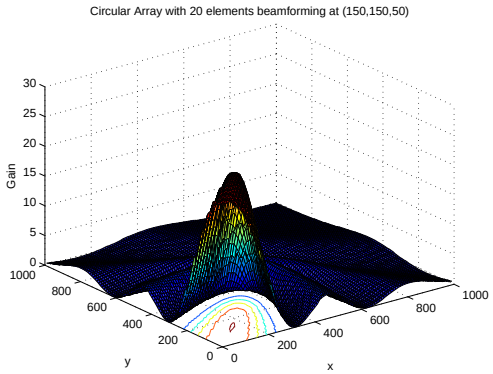

Fig. 3. Gain with a 20-element circular array pointing to (1.5m,1.5m,0.5m).

III. Achievable Data Rates

The use of highly directional antennas at 60GHz gives us the opportunity to exploit the spatial locality of a beam. In this section, we look at the problem of determining the *protocol-independent* maximum and average throughput of a 60GHz system when the AP as well as users are equipped with identical smart antennas. The key to maximizing throughput is to allow multiple links to operate simultaneously such that the aggregate data rate is maximized. For this, we will need multiple beamforming modules as well as radios at the AP – one per link. For the purposes of calculating the maximum and average obtainable throughout, we assume perfect channel sharing (e.g., using TDMA) in each beam.

A. Linear Array

Figure 1 shows the gain from the AP to the user (beamforming at the AP) for a linear antenna array. As is evident, the rotational symmetry (about the array axis) causes the region of highest gain to be spread in a narrow strip across the floor of the room (when viewed on the x-y plane). Indeed, if we sweep the beam across all the angles, we will see this strip move in the direction of the y-axis. This behavior gives us a natural way to think about constructing multiple spatial channels simultaneously. As an example, given two modules, we can form one beam at some angle θ_1 and the other at θ_2 such that the interference between these two beams is low enough to maximize throughput. In other words, the gain of the transmission at angle θ_1 *in the direction* of θ_2 should be very small, and vice versa. This constraint can be naturally extended to the case when we have k modules available at the AP allowing us to form up to k links. One other consideration we need to keep in mind is that *the entire room needs to be covered*. Therefore, our approach is to *sweep* the beams across the room in discrete time steps that gives us a STDMA (Spatial Time Division Multiple Access) schedule.

It is evident that, given k beamforming modules, the problem of where to point each beam and then sweeping the beams to cover the room has a large number of possible solutions (given the continuous nature of the variables such as the angle). The algorithm that we developed, after a great deal of experimentation, is to discretize the problem by first identifying *regions* of coverage and using these as the resource to be allocated to different beamforming modules. To explain the idea, let us consider a room of dimension 10m X 10m X 3m. The linear array is located in the center of the ceiling at (5m, 5m, 3m) and aligned parallel to the x-axis. We begin by forming a beam to a user located at (0.1m, 5m, 0.5m). We define region 1 as all the locations that are *within 3 dB* of the maximum gain. Region 2 is now formed by aiming the beam at another point (x m, 5m, 0.5m) and including all locations that are within 3 dB of the maximum gain of this beam. The value of x is such that the overlap between region 1 and region 2 is very small and these two regions are right next to one another. This process is continued until we cover the entire room. Figure 4 shows the 21 regions obtained for the example room we are considering. Figure 5 plots the corresponding antenna gain when we point the beam at the center of each region. The gain shown in the 2D plot corresponds to the gain seen along the line connecting points (0m, 5m, 0.5m) and (10m, 5m, 0.5m) – the line running along the center of the room parallel to the x-axis and 0.5m above the floor. Note that the gain seen in region i from a beam formed towards region $i+1$ (or $i-1$) is less than 3 dB (in Figure 5 this is shown via the intersection of the horizontal line with the gain plot).

For a given STDMA schedule, we compute the *maximum* and *average* obtainable throughput as follows. The maximum throughput is the mean of the maximum throughput seen

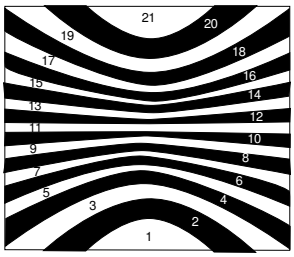

Fig. 4. The 21 regions formed with a linear array.

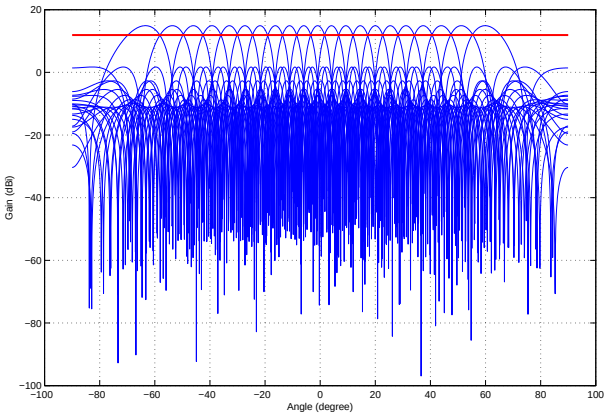

Fig. 5. The gain seen at the 21 regions formed with a linear array.

in each region. The maximum throughput in a region will typically only occur at a few points. This is the value used for that region. The average throughput for the WLAN is the mean of the average throughput's seen in each region. The average throughput in a region is computed by randomly uniformly placing a user in the region and finding the mean data rate. To compute the data rates, we use system parameters from Tables I and II.

The STDMA schedule is found simply as follows. For k modules, we can simultaneously form k beams. To ensure that interference between beams is minimized, we maximize the angular separation between the beams. For example, if $k = 3$, we have the following schedule: {(1,8,15), (2,9,16), (3,10,17), (4,11,18), (5,12,19), (6,13,20), (7,14,21)}. Thus we use 7 slots and in each we simultaneously have 3 links. The schedule for $k = 8$ is: {(1,4,7,10,13,16,19,21), (2,5,8,11,14,17,20), (1,3,6,9,12,15,18,21)}. As we can see, when the number of regions is not perfectly divisible by k, the separation of regions in the same time slot is not uniform. Given r regions and k modules, the separation between regions in the same time slot is either $\lfloor \frac{r}{k} \rfloor$ or $\lceil \frac{r}{k} \rceil$.

Room dimensions	10m x 10m x 3m
AP location	Center of ceiling
Transmit power	10 dBm
Bandwidth	640 MHz
Modulation	Table II
No. antenna elements AP and user	$M = 20$
No. Modules k at AP	1 – 21 (Linear)
	1 – 49 (Circular)

TABLE I
EXPERIMENTAL PARAMETERS.

Modulation	*Code Rate*	*Min* E_b/N_0 *for* $P_b \leq 10^{-6}$	*Rate (Mbps)*
64-QAM	3/4, 1/2	22.65 dB	1080, 960
16-QAM	3/4, 1/2	19.1 dB	720, 480
QPSK	3/4, 1/2	16.7 dB	360, 240
BPSK	3/4, 1/2	11.45 dB	180, 120

TABLE II
BIT PER SECOND FOR DIFFERENT MODULATION SCHEMES [10].

In our experiments, we also use the nulling capability of smart antennas. Thus, given k modules, we form k simultaneous beams – each module beamforms in one direction and nulls the remaining $k-1$ directions. For instance, if $k = 3$ and regions (1,8,15) are active simultaneously, the module that beamforms towards region 1 also nulls the center point of regions 8 and 15, and so on. An interesting observation we can make is that since our antennas have $M = 20$ elements, we can potentially form 19 nulls per module. Thus, if $k < M$ and we form $k-1$ nulls as described, we still have the capability to form an additional $M-k$ nulls per module. The question is where to form the additional nulls, and whether this is a useful thing to do.

We research this question in some detail. Consider Figure 6 where we beamform towards region 1 and null the center of region 11 and we only use $k = 2$ beamforming modules. If we look at the gain at areas close to the null, we see a steep increase in gain – the center of region 11 is at -48 dBi while the edges are at -30 dBi. This means that even if we null the center of any region from Figure 4, it is likely that there will be significant gain as we go to the boundaries of that region, which will result in more interference. This observation means that given the opportunity to form additional nulls, we should form more than one null per region at different angular locations such that interference in that region is reduced overall. In Figure 7 we plot the case when we form $M-1$ nulls in region 11 (each null is incrementally located a small fraction of a radian off center) while beamforming to region 1 and vice versa. We see that the interference from beamforming at region 1 towards region 11 is now well below -100 dBi across the entire span of region 11 (and vice versa). This clearly indicates that forming multiple nulls within a region is a beneficial thing to do.

We compared the cases when modules only form $k-1$ nulls and when modules form $M-1$ nulls. The algorithm we used to allocate the additional $M-k$ nulls is as follows. For each of the $k-1$ nulling directions, we allocate $\lfloor \frac{M-k}{k-1} \rfloor$ additional nulls. These nulls are then formed at angles $\pm\epsilon, \pm 2\epsilon, \cdots$ about the center of the region until we form all the allocated nulls. The performance of the algorithm for different values of ϵ are somewhat different and in our plots we report on only two extreme values, $\epsilon = 0.0005, 0.03$ radians. Another method we consider is called *uniform* where we first find the beamwidth of a region (i.e., the 3 dB boundary) and then distribute the

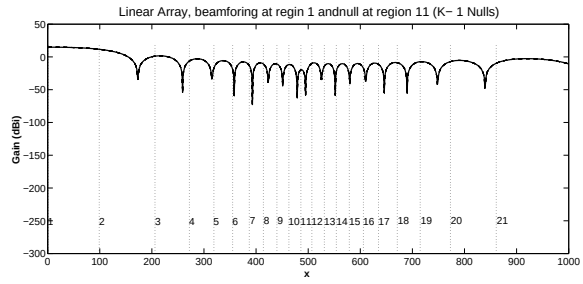

Fig. 6. Beamform to region 1, place a single null in region 11.

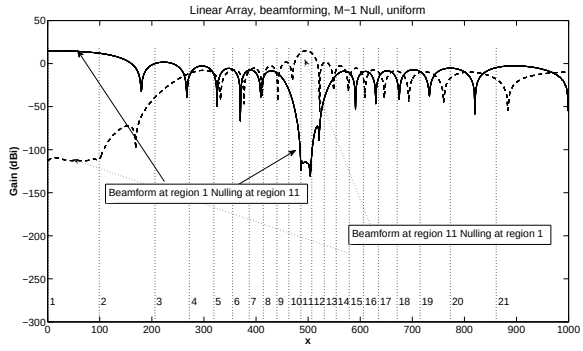

Fig. 7. Forming 19 nulls in each region.

$\lfloor \frac{M-1}{k-1} \rfloor$ nulls equally spaced (in an angular sense) in the region. Note that in all experiments the user also beamforms towards the AP using an identical antenna array. However, the user does not form nulls since interference from uplink transmissions from other users is negligible.

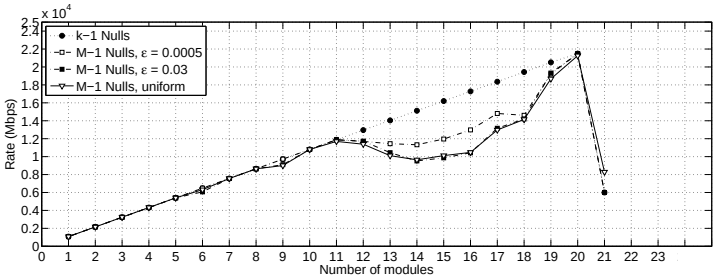

Fig. 8. Maximum throughput for the linear array.

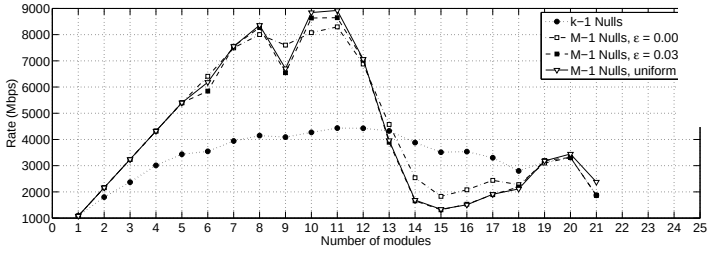

Fig. 9. Average throughput for the linear array.

Figure 8 plots the maximum throughput obtained for the room we are considering as a function of the number of beamforming modules available, k. Figure 9 plots the average throughput. Initially, as we increase the number of modules, the throughput (maximum and average) also increases linearly as seen in the two figures. This is because the mutual interference is very low and thus we are simply gaining throughput as we add modules. Let us now look at Figure 8 in more detail. It is interesting to note that the maximum throughput of 22 Gbps is obtained when using 20 modules and forming $k-1=19$ nulls. Indeed, the maximum data rate is equal to the number of modules multiplied by 1.08Gbps. Furthermore, forming $k-1$ nulls is the best choice rather than forming $M-1$ nulls! The reason for this is that since we are only finding the best SINR per region (a single point), when we form $M-1$ nulls per region, the main beam shifts and flattens slightly resulting in lower desired signal levels. There appears to be little difference in maximum throughout for the two values of ϵ selected.

If we look at the average throughput in Figure 9, however, the story is quite different. The maximum throughput of 9 Gbps is obtained at 10 and 11 modules when we form $M-1=19$ nulls. Indeed, forming only $k-1$ nulls causes the average throughput to reduce in half. The reason that forming more nulls is better is simply that we reduce interference levels in the *region as a whole* from other beams. Since the average is computed by assuming a uniform random user placement over the entire region, more nulls provide a greater overall benefit. Increasing the number of modules beyond 13 appears to be detrimental as we increase the total interference seen and thus lower the data rate. In Figure 10 we plot the signal levels at each region when using $k=14$ modules and beamforming at region 1. There is one plot for the case when forming $M-1$ nulls using the uniform algorithm and for the case when forming $k-1$ nulls. As is clear, the desired signal in region 1 is much higher when we only form $k-1$ nulls. The reason is that as we form more and more nulls, the main beam flattens out and spreads more. Therefore, there is a optimal number of nulls one can form that trades off the benefits of reducing interference with the cost of reducing the desired signal strength.

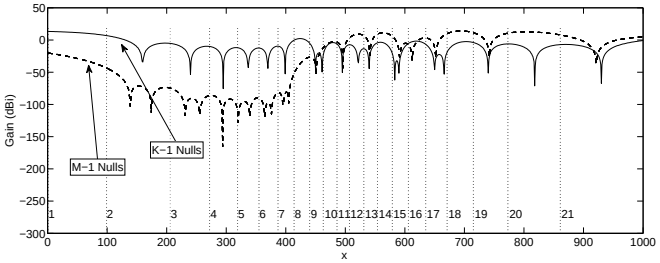

Fig. 10. Comparison of the desired signal levels when using 14 modules.

B. Circular Array

Determining the maximum achievable throughput for the circular array case follows the same steps as in the case of the linear array. That is, we first identify regions and then

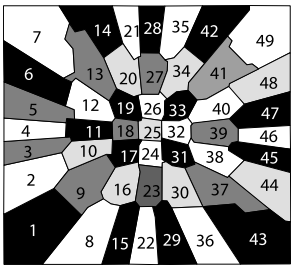

Fig. 11. The 49 regions formed with a circular array.

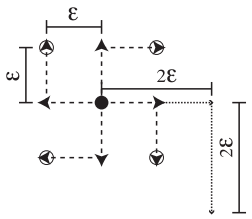

Fig. 12. Epsilon walk algorithm.

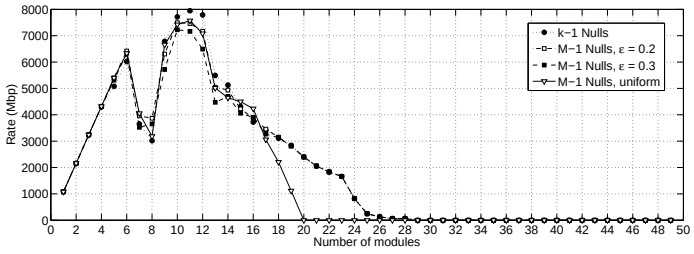

Fig. 13. Maximum throughput with a circular array.

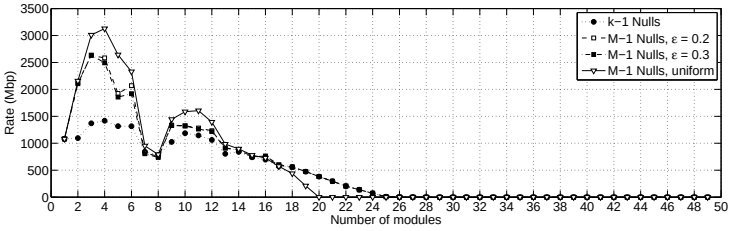

Fig. 14. Average throughput with a circular array.

construct schedules given k modules. Figure 11 shows the regions created by applying the constraint that a region's boundary is 3 dB below the maximum gain within the region. As we can see, the regions formed are not uniform and are of different sizes. For the 10m X 10m room, we get 49 distinct regions. Observe that as we get further away from the center of the room, the regions get elongated. This happens because the beam hits the floor obliquely.

As in the case of the linear array, the problem of computing the maximum and average throughput relies on constructing appropriate STDMA schedules with k modules such that the room is completely covered. There are many different approaches one can take to find the best possible throughput (indeed, the problem of finding the optimal throughput can be shown to be NP-complete). However, we instead use the following algorithm for its computational simplicity. Given k modules, we compute $d = \lfloor \frac{49}{k} \rfloor$. The schedule then is: $\{(1,\ d+1,\ 2d+1,\ \cdots,\ (k-1)d+1),\ (2,\ d+2,\ 2d+2,\ \cdots,\ (k-1)d+2),\ \cdots,\ (\text{d},\ 2d,\ 3d,\ \cdots,\ kd)\}$. If the number of regions is not perfectly divisible by k then we will need an additional time slot to accommodate the remaining regions.

The problem of forming nulls is similar to the discussion we had previously. Thus, we consider the case when we form only $k-1$ nulls given k modules and when we form $M-1$ nulls. However, the algorithms for forming $\lfloor \frac{M-1}{k-1} \rfloor$ nulls per region are different. The first algorithm, called ϵ-walk is illustrated in Figure 12. The idea is that we walk along a grid of side ϵ around the center of a region and use the vertices as locations for the additional nulls. The second algorithm places nulls uniformly randomly in the entire region to be nulled.

Figure 13 plots the maximum throughput for the circular array. We note that the maximum throughput of 8 Gbps is obtained when we have 11 modules. Interestingly, forming more than $k-1$ nulls does not have much of an impact. The reason is the same as in the linear case where forming more nulls does not improve maximum throughput as it is computed at one point per region (the point that has the highest SINR). However, in comparing these results with those in Figure 8, observe that the maximum throughput for the circular array is far below the linear case, even though we expect the circular array to provide a narrower beam. The reason for this difference is made clear if we look at Figures 1 and 3. The SIR for a link can be shown to be proportional to the ratio G_t/G_I where G_t is the gain of the transmitter in the direction of the receiver and G_I is the gain of the interferer in the direction of the receiver. Note that in our case, the desired transmitter as well as the interferer are co-located (we simply use different modules for beamforming and nulling). In the case of the linear array from Figure 1, $G_t = 13.72$ dBi and $G_I = -3.09$ dBi (on average). Thus the SIR is proportional to $G_t/G_I = G_t$ (dBi)$-G_I$ (dBi)$= 16.81$ dBi. In case of the circular array the values we have are $G_t - G_I = 14 - 1.68 = 12.32$ dBi. The difference in SIR between the linear array and the circular array is thus more than double (3 dBi) and this explains why the linear array shows greater maximum throughput.

Figure 14 plots the average throughput for the circular array. We obtain a maximum of 3.25 Gbps when using 4 modules and forming $M-1$ nulls uniformly spaced in the regions being nulled. The ϵ-walk algorithm does not perform as well since the nulls are being clustered about the center of the region which leaves the remaining parts of the region to have non-trivial gain values. The difference between forming only $k-1$ nulls and $M-1$ nulls is more than double, as in the linear case.

The wavy behavior of the maximum throughput plot and the average throughput plot is an artifact of the manner in which the STDMA schedules are constructed. When $k = 8$, with 49 regions, we get $\lfloor 49/8 \rfloor = 6$. Thus, regions (1, 7, 13, 19, 25, 31, 37, 43) are assigned to the same time slot. As we can see

in Figure 11, all regions with the exception of 1 lie next to one another along a diagonal. Thus, even though we perform nulling, the SIR is going to be poor.

IV. Link Reliability

As we noted in Section I, the 60GHz spectrum is particularly susceptible to oxygen absorption and higher attenuation when encountering different materials in its path. This means that links can be broken by mobility as well as partitions etc. We explore the idea of using reflectors to mitigate these problems. Some materials, such as wire mesh glass [6], have excellent reflective properties at 60GHz and only attenuate the signal by 3 dB for most angles of incidence. Therefore, one inexpensive way to mitigate dead spots in a room is to strategically place sections of this material on the walls and reflect signals off this to provide coverage in the dead spots. The drawback of this scheme is that it is not adaptive. However, for room architectures that do not change much, this is an inexpensive way to solve the coverage problem.

Let us examine the problem of integrating reflectors into the STDMA schedules developed for the linear array. In the case of a linear array, say we were to place a reflector on one wall (assume the array axis is parallel to the x-axis and we place the reflector on the wall parallel to the x-z plane). This has the effect of reflecting some regions back into the room. Consider Figure 15 where we assume that two walls parallel to the x-z plane are covered by a reflector over the bottom 1.5m. As we can see, each region is reflected back into the room.

We evaluate the data rate achieved with a linear array for three different cases when entire regions are a dead spot. The three cases considered are that either region 1 or region 4 or region 13 are dead spots. We used 7 modules and formed $M-1$ nulls from each module to maximize average throughput. Figure 16 plots the average data rate in each region. As expected, average throughput in all LoS regions remains high while the regions that are dead spots show lower average throughput. The reason the throughput is lower is that the signal path length is longer when going via the reflector and because of attenuation of 3 dB at the reflector. The throughput of region 13 is much lower than that of regions 1 and 4 because the total interference in region 13 is higher – region 13 is in the center of the room and is thus susceptible to more interference from direct as well as reflected paths.

V. Conclusions

The results in this paper show that the antenna geometry has a significant impact on achievable throughput. We show that there is an optimal number of beamforming modules that maximize average throughput. Adding more modules only serves to increase interference and reduce throughput. Finally, we explore the potential of passive reflectors in the room to improve coverage in dead spots. We show that appropriately placed reflectors can increase coverage though at a reduced data rate. The results presented in this paper can be used in the design of MAC protocols that are specific to this frequency band. This is part of our future work.

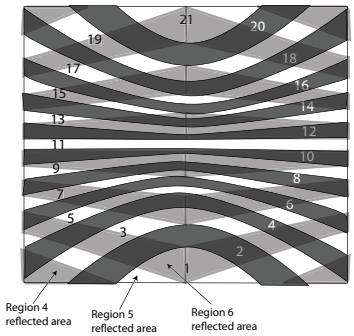

Fig. 15. Reflected regions assume two walls are reflective at the bottom 1.5m.

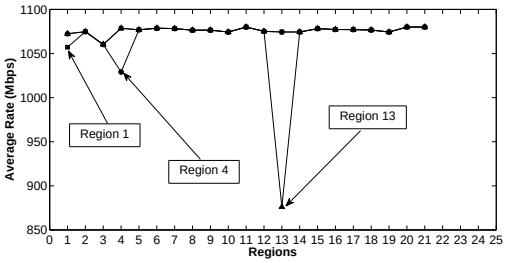

Fig. 16. Data rate for three dead spot scenarios (Linear Array).

References

[1] S. E. Alexander and G. Pugliese. Cordless communications within buildings: Results and measurements at 900mhz and 60ghz. *British Telecom Technology Journal*, 44(10):99 – 105, Oct. 1996.

[2] C. R. Anderson and T. S. Rappaport. In-building wideband partition loss measurements at 2.5 and 60 ghz. *IEEE Trans. on Wireless Communications*, 3(3):922 – 928, May 2004.

[3] J-P. Ebert et. al. Paving the way for gigabit networking. In *Global Communications Newsletter*, April 2005.

[4] G. Fettweis and R. Irmer. Wigwam: system concept development for 1 gbit/s air interface. Wireless OWrld, Rsearch Forum, 2005.

[5] E. Grass, M. Piz, F. Herzel, and R. Kraemer. Draft phy proposal for 60ghz wpan: Ieee p802.15 wg on wpans, November 2005.

[6] B. Langen, G. Lober, and W. Herzig. Reflection and transmission behavior of building materials at 60ghz. In *IEEE PIMRC'94*, pages 505–509, 1994.

[7] C. P. Lim, R. J. Burkholder, J. L. Volakis, and R. J. Marhefka. Propagation modeling of indoor wireless communications at 60 ghz. In *IEEE Antennas and Propagation Society International Symposium*, pages 2149 – 2152, 2006.

[8] M. Marcus and B. Pattan. Millimeter wave propagation: spectrum management implications. *IEEE Microwave Magazine*, June 2005.

[9] S. Singh, F. Ziliotto, U. Madhow, E. M. Belding, and M. J. W. Rodwell. Millimeter wave wpan: Cross-layer modeling and multi-hop architecture. In *IEEE INFOCOM (Minisymposium)*, pages 2336 – 2340, May 2007.

[10] Bernard Sklar. *Digital Communications*. Prentice Hall, 2005.

[11] P. Smulders. Exploiting the 60ghz band for local wireless multimedia access: prospects and future directions. *IEEE Communications Magazine*, pages 140 – 147, January 2002.

[12] H. Xu, V. kukshya, and T. Rappaport. Spatial and temporal characteristics of 60ghz indoor channels. *IEEE Journal in Selected Areas in Communications*, 20(3):620 – 630, April 2002.